1   **Super Enhancer-driven LncRNA UNC5B-AS1 Inhibits Inflammatory Phenotypic**

2   **Transition in Smooth Muscle Cells via Lactylation Modification**

3   Xiangrui Zhu[1], Xiangming Pang[1], Xiaoying Wang[2], Xiaoyu Guan[5], Zhaosi Wang[1], Lixin

4   Zhang[1, 3], Xiaodong Zheng[3], Fei Li[4], Jian Mei[1], Langlin Ou[1], Yuxiang Liu[1], Zitong Meng[1],

5   Yingli Chen[1], Cui Ma[1, 3*]

6   1 College of Medical Laboratory Science and Technology, Harbin Medical University (Daqing),

7   Daqing 163319, P. R. China.

8   2 College of Pharmacy, Harbin Medical University (Daqing), Daqing 163319, P. R. China.

9   3 Central Laboratory of Harbin Medical University (Daqing), Daqing 163319, P. R. China.

10   4 College of Basic Medicine, Harbin Medical University (Daqing), Daqing 163319, P. R. China.

11   5 College of Pharmacy, Harbin Medical University, Harbin 150081, P.R. China.

12   **Short title:** UNC5B-AS1: A Target for Inflammation in PASMCs

13   *Corresponding author: Cui Ma, Email: macui0804@sina.com, Central Laboratory of Harbin

14   Medical University (Daqing), Daqing 163319, P. R. China.

15   **Total word count:7401**

16

Abstract

Background: The phenotypic transition of pulmonary artery smooth muscle cells (PASMCs) is a central pathological alteration in pulmonary artery remodeling that contributes to pulmonary hypertension (PH). The specific role of long noncoding RNAs (lncRNAs), especially super enhancer (SE)-driven lncRNAs, in the phenotypic transformation of PASMCs induced by hypoxia remains unclear. The objective of this study is to determine the mechanistic role of the super enhancer-driven LncRNA UNC5B-AS1 in phenotypic transformation of PASMCs and hypoxia-induced vascular remodeling.

Methods: The lncRNA UNC5B-AS1 regulated by super-enhancers was identified in hypoxic human PASMCs through RNA sequencing and H3K27ac ChIP sequencing. Overexpression of lncRNA UNC5B-AS1 in human PASMCs was performed to elucidate its role in the pathogenesis of PH. A conserved functional fragment of lncRNA UNC5B-AS1 was used for the treatment of mouse PH.

Results: In PASMCs, we have identified a SE-driven lncRNA called UNC5B-AS1 that regulates phenotype transition. It is transcriptionally activated by the transcription factor FOXP3. We demonstrate that UNC5B-AS1, as a molecular scaffold in mitochondria, stabilizes the interaction between LRPPRC, which is rich in leucine, and oxidative respiratory chain complex IV. This complex regulates the lactylation modification level of upstream promoter regions of inflammatory genes IL-1β, IL-6, and TNF-α by influencing the glycolytic pathway in PASMCs under hypoxic conditions, ultimately affecting the inflammatory phenotype transition of PASMCs.

Conclusions: Our findings identify the SE-driven lncRNA UNC5B-AS1 as a novel regulatory

39 factor in hypoxia-induced phenotypic switch of PASMCs, and suggest that overexpression of

40 UNC5B-AS1 may represent a promising therapeutic strategy for PH.

41 **Key Words:** Super Enhancer; Long noncoding RNA; Smooth Muscle Cells; Inflammatory

42 Phenotypic; Pulmonary Hypertension; Lactylation Modification

43
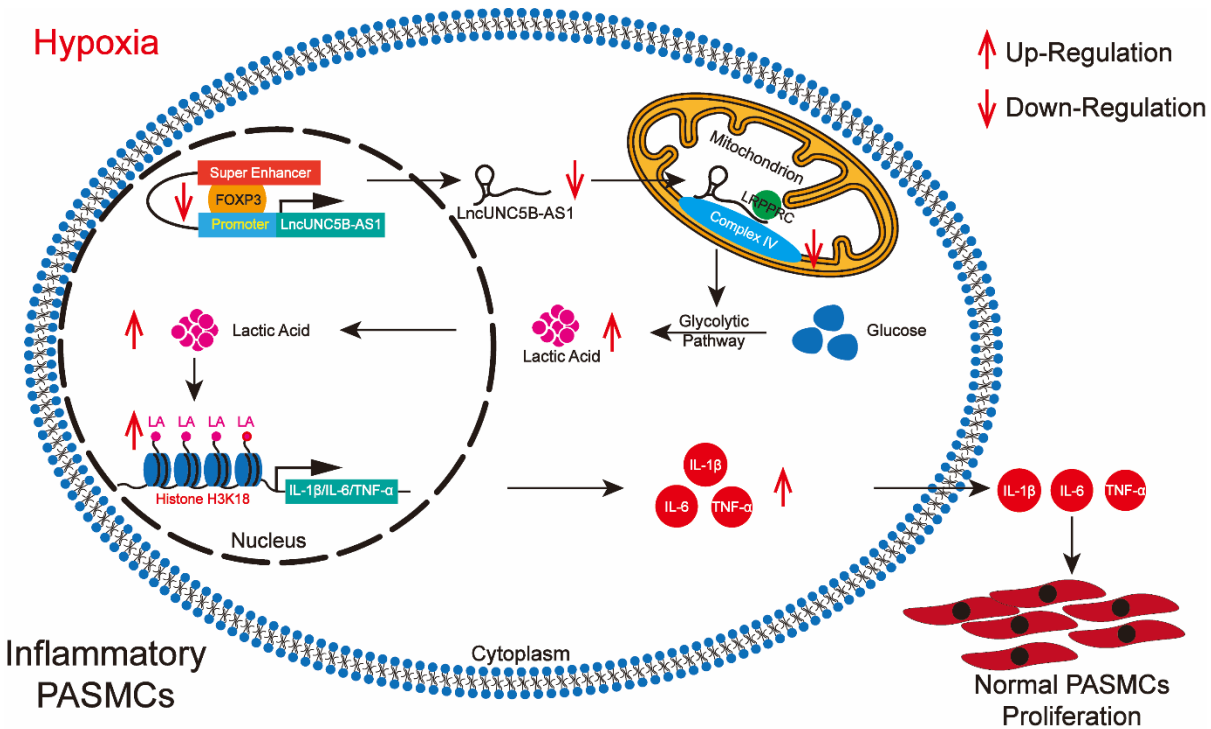
Non-standard Abbreviations and Acronyms	
UNC5B-AS1	UNC5B antisense RNA 1
PASMCs	Pulmonary Artery Smooth Muscle Cells
PH	Pulmonary Hypertension
lncRNA	Long Noncoding RNA
SE	Super Enhancer
ChIP	Chromatin Immunoprecipitation
LRPPRC	Leucine-Rich PPR Motif-Containing Protein
FOXP3	Forkhead Box Protein P3

IL	Interleukin
TNF-α	Tumor Necrosis Factor Alpha
OPN	Osteopontin
KLF4	Krüppel-Like Factor 4
CNN1	Calponin-1
SM22α	Smooth Muscle Protein 22-alpha
HKII	Hexokinase II
PKM2	Pyruvate Kinase M2
ECAR	Extracellular Acidification Rate
CM	Conditioned Medium
SuHx	Sugen5416/Hypoxia
AAV5	5 Adenovirus-Associated Virus
H&E	Hematoxylin And Eosin Staining
UA1CF	UNC5B-AS1 Conserved Fragment
RV/LV	Right Ventricle/Left Ventricle
RVSP	Right Ventricular Systolic Pressure
PAAT	Pulmonary Artery Acceleration Time
PAVTI	Pulmonary Artery Velocity-Time Integral
EF	Ejection Fraction

Introduction

The pathology of pulmonary hypertension (PH) is complex and associated with cardiac,

pulmonary, and systemic diseases that contribute to morbidity and mortality[1]. PH is

4

47 characterized by inflammation, pulmonary vascular remodeling, and pulmonary vascular

48 embolism leading to elevated pulmonary arterial pressure and resistance, right ventricular

49 dysfunction, left ventricular compression, and subsequent heart failure[2,3]. The remodeling

50 process occurs throughout the pulmonary arterial vasculature and involves medial thickening,

51 which is driven by increased proliferation and hypertrophy of pulmonary artery smooth muscle

52 cells (PASMCs), its principal cellular component[4]. However, there is heterogeneity among

53 PASMCs, which can exhibit markedly different changes in proliferative, inflammatory, and

54 extracellular matrix production during remodeling[5-7]. Typically, PASMCs express high levels

55 of contractile proteins such as α-smooth muscle actin (α-SMA), calponin, SM22α and other

56 differentiation markers, which is accompanied by a low rate of proliferation[5,8,9]. Under

57 pathological conditions, PASMCs acquire inflammatory cell markers and release inflammatory

58 cytokines, such as interleukin (IL)-1β, IL-6 and tumor necrosis factor (TNF)-α, contributing to

59 the proinflammatory environment, which is followed by vessel injury and remodeling[10]. These

60 findings suggest that the inflammatory phenotypic transition of PASMCs can contribute to the

61 development of PH.

62 Long noncoding RNAs (lncRNAs) are non-protein-coding transcripts with lengths greater

63 than 200 nucleotides[11]. An increasing number of studies have shown that lncRNAs play

64 important roles in diverse cellular processes, including proliferation[12], apoptosis[13], migration[14],

65 invasion[15], chromatin remodeling[16], metabolism[17], and immune escape[18]. Super enhancers

66 (SEs) are a widespread class of chromatin regulatory elements in the genome that are closely

67 associated with the expression levels of specific genes[19]. LncRNAs driven by SEs are lncRNAs

68 expressed near SEs that regulate gene expression through interactions with SEs. In gliomas,

69   the SE-driven lncRNA TMEM44-AS1 promotes tumor cell growth through the formation of a

70   positive feedback loop with MYC[20]. The lncRNA NEAT1 has been identified as an SE-driven

71   lncRNA that controls the lineage fate of bone marrow mesenchymal stem cells (BMSCs) during

72   skeletal aging by affecting mitochondrial function[21]. Moreover, lncRNA CARMN has been

73   confirmed to be driven by an SE in vascular smooth muscle cells and is involved in maintaining

74   the contractile phenotype of smooth muscle cells[22]. However, the mechanism of SE-driven

75   lncRNAs in PASMCs inflammatory phenotypic transition and PH development needs to be

76   further examined.

77   Emerging evidence shows that lactate has regulatory functions in physiologic and

78   pathologic cells and induces dramatic changes in gene expression, suggesting that lactate is not

79   simply a waste product of glycolysis[23]. In response to hypoxia, cells undergo metabolic

80   reprogramming by inhibiting oxidative phosphorylation and enhancing glycolysis, thereby

81   stimulating the production of lactate[24]. Recent studies indicated that hypoxia induced

82   intracellular lactate production and increased histone Kla but not Kac levels in MCF-7 cells[23].

83   Lactate-derived lactylation of histone lysine residues is an epigenetic modification that directly

84   stimulates gene transcription[25]. Histone lactylation modification can influence the transition of

85   inflammatory macrophage phenotypes, thereby impacting inflammation levels and

86   participating in the progression of related diseases[25,26]. Thus, controlling the glycolytic switch

87   via lactylation suggests novel therapeutic opportunities to treat PH.

88   In this study, we showed for the first time that lncRNA UNC5B antisense RNA 1(UNC5B-

89   AS1, Chr10q22.1) was regulated by SEs in PASMCs. It is transcriptionally activated by the

90   transcription factor forkhead box protein P3 (FOXP3). Our data indicated that UNC5B-AS1

6

91   served as a molecular scaffold in mitochondria and interacted with leucine-rich PPR motif-

92   containing protein (LRPPRC) and mitochondrial complex IV. Under hypoxic conditions, the

93   loss of UNC5B-AS1 expression impaired mitochondrial oxidative phosphorylation, leading to

94   abnormal activation of glycolysis. The accumulation of lactate due to the activation of

95   glycolysis in hypoxia, affected the lactylation of inflammatory factor promoters in PASMCs

96   and ultimately promoted the transition of PASMCs to an inflammatory phenotype and

97   contributed to the progression of PH.

98   **Methods**

99   **Animal**

100   This study used adult male C57BL/6 mice (6-9 weeks old) obtained from the Experimental

101   Animal Center of the Second Affiliated Hospital of Harbin Medical University. All

102   experimental procedures have obtained approval from the Ethics Committee of Harbin Medical

103   University (HMUDQ20230831001). All animal studies were conducted in compliance with the

104   National Institutes of Health (NIH) guidelines for the care and use of laboratory animals. The

105   RNA cloning constructs, and serotype 5 adenovirus-associated virus (AAV5) were synthesized

106   by GeneChem (China). After randomization, the mice were divided into groups and

107   intranasally infected with 10^{11} genome equivalents of AAV5 vector solution diluted with 20 μL

108   of Hank's balanced salt after isoflurane anesthesia. After 14 days, the mice were assigned to

109   normoxia (21% O_2) and hypoxia (10% O_2) conditions, as described in previous studies[27]. In

110   the Sugen hypoxia model, the mice were injected once per week with the VEGF inhibitor

111   SU5416 (Med Chem Express, USA) at a concentration of 20 mg/kg. Subsequently, the mice

112   were subjected to 3 weeks of hypoxia (10% O_2) followed by 2 weeks of reoxygenation (21%

113   O_2). The control group was maintained in a normal oxygen environment, and the oxygen

114   concentration was continuously monitored for 5 weeks using an oxygen analyzer (BioSpherix,

115   USA). After constructing the model, euthanasia was performed on mice using a small animal

116   euthanasia system (Yuyan Instruments, China) by inhalation of 100% CO_2, followed by

117   cervical dislocation as a secondary confirmation of death. Lung tissue was collected for further

118   experiments. The right ventricular (RV) hypertrophy index (RV/(LV+S)), is calculated by

119   dividing the weight of the right ventricular free wall by the sum of the weight of the septum

120   plus the left ventricular free wall.

121   **Small Animal Echocardiography and Right Ventricular Systolic Pressure**

122   After the completion of hypoxia and SU5416 treatment, the mice underwent

123   echocardiography using the Vevo2100 imaging system equipped with an 18 to 38MHz

124   transducer probe (VisualSonics, Canada), as described previously[28]. Mice were anesthetized

125   using a desktop anesthesia machine (Harvard Apparatus, USA) with inhalation of a

126   concentration of 1% to 3% isoflurane. The mice were placed on a preheated imaging platform

127   and the respiratory rate was continuously monitored throughout the entire echocardiography

128   process. The pulmonary artery acceleration time (PAAT) and pulmonary artery velocity-time

129   integral (PAVTI) were measured using pulse wave Doppler. Transthoracic echocardiography

130   was performed in the short-axis view at the level of the sternum to measure left ventricular

131   ejection fraction at end-diastole and end-systole. All measurements were performed by

132   experienced researchers, and data analysis was conducted in a blinded manner using Vevo2100

133   software. Right ventricular systolic pressure was measured using the PowerLab monitoring

134   system (AD Instruments, USA). The pressure catheter (Scisense Inc) was inserted into the right

135 ventricular vein via the superior vena cava, and right ventricular systolic pressure was

136 continuously recorded for 10 to 30 minutes.

137 **ChIP-seq**

138 ChIP-seq was performed by Guangzhou Epibiotek Co., Ltd. Briefly, the cells were cross-

139 linked with 1% formaldehyde for 10 minutes, followed by quenching the cross-linking reaction

140 with 0.125M glycine. The cells were then frozen on dry ice and stored until further use. After

141 isolating the cell nuclei, the chromatin was sheared to fragment it into sizes ranging from 200

142 to 500 bp. 5 µg of anti-H3K27ac antibody (Cell Signaling) was incubated overnight with the

143 fragmented chromatin. Protein A magnetic beads were used to capture immune complexes. The

144 chromatin was eluted in reverse cross-linking buffer followed by incubate the tube at 65°C for

145 3h. After digestion with RNase and Proteinase K, the fragments were purified and quantified.

146 ChIP DNA was processed for library generation using the QIAseq Ultralow Input Library Kit

147 (QIAGEN) following the manufacturer's protocol. After library construction, the samples were

148 subjected to sequencing analysis.

149 **RNA-seq**

150 PASMCs cultured under normoxia/hypoxia conditions were harvest or RNA-seq. Total RNA

151 was isolated using TRIzol reagent (Thermo Fisher Scientific, Massachusetts) according to the

152 manufacturer's protocol. VAHTS Stranded mRNA-seq Library Prep Kit for Illumina V2

153 (Vazyme Biotech, NR612-02) was used for library preparation according to the instructions.

154 The libraries were then sequenced on the Illumina NovaSeq 6000 platform by Epibiotek Co.,

155 Ltd. in Guangzhou.

156 **Statistical Analysis**

157   The statistical analysis was performed using GraphPad Prism 8 software. Prior to statistical

158   testing, the data were checked for normality and homogeneity of variances (F test). Student's

159   t-test (unpaired) was used for analyzing data with equal variances in two groups, while Welch's

160   corrected t-test was used for analyzing data with unequal variances in two groups. One-way

161   analysis of variance (ANOVA) with Tukey's post hoc test was used to compare multiple groups

162   with equal variances, while Brown-Forsythe and Welch's ANOVA with Tamhane T2 post hoc

163   test were used to compare multiple groups with unequal variances. Nonparametric analysis was

164   used for non-normally distributed data, including Mann-Whitney U test or Kruskal-Wallis test

165   for two group analysis, followed by Dunn's post hoc test for >2 groups. Data are presented as

166   mean $\pm$ SEM, and a P value of <0.05 is considered statistically significant.

167   **Results**

168   **UNC5B-AS1 is a super enhancer-driven lncRNA that is downregulated by hypoxia.**

169   To identify differentially expressed lncRNAs in PH, we performed RNA-seq and

170   H3K27ac ChIP-seq assays on PASMCs subjected to normoxia/hypoxia. Our results revealed

171   significant downregulation of UNC5B-AS1 under hypoxic conditions (Fig.1A, B). H3K27ac

172   ChIP-seq analysis was used to identify super enhancers in the upstream regulatory regions of

173   genes, the hockey-stick plot demonstrated increased super enhancer activity upstream of

174   UNC5B-AS1 under normoxic conditions (Fig.1C). Similarly, there was significantly increased

175   abundance of H3K27ac modification upstream of the gene in normoxic conditions (Fig.1D).

176   We further validated the significant downregulation of UNC5B-AS1 under hypoxic conditions

177   in PASMCs (Fig.1E), and in response to JQ1 (an effective BET bromodomain inhibitor)

178   treatment, the expression of UNC5B-AS1 was significantly inhibited after the chromatin

179   interaction was suppressed (Fig.1F). Fluorescence in situ hybridization (FISH) indicated

180   cytoplasmic localization of UNC5B-AS1 in PASMCs (Fig.1G). Taken together, these findings

181   suggest that UNC5B-AS1 is regulated by super enhancers in PASMCs and that its expression

182   is downregulated and localized in the cytoplasm under hypoxic conditions.

183   FOXP3 regulates the expression of UNC5B-AS1 through chromatin remodeling.

184   UNC5B-AS1, which is a super enhancer-regulated lncRNA that is downregulated under

185   hypoxic conditions, motivated us to further investigate the upstream regulatory mechanisms

186   driving its expression. We used three bioinformatics tools to screen for potential transcription

187   factors that could regulate UNC5B-AS1 expression (Fig.S1A left). Based on the number and

188   binding agent of the binding sites within the upstream promoter region of UNC5B-AS1, we

189   identified FOXP3 as a key transcription factor that regulates UNC5B-AS1 expression (Fig.S1A

190   right). Immunoblotting showed that FOXP3 was downregulated under hypoxic conditions

191   (Fig.2A). Subsequently, based on the H3K27ac ChIP-seq results, we divided the upstream

192   super enhancer region of UNC5B-AS1 into three segments (E1-E3, Fig.2B). ChIP-qPCR

193   experiments using H3K27ac (Histone 3 Lysine 27 Acetylation, super-enhancer marker),

194   H3K4me1 (Histone 3 Lysine 4 Monomethylation, enhancer marker), and FOXP3 antibodies

195   revealed that FOXP3 had a strong binding affinity to segment E2 of the UNC5B-AS1 upstream

196   super enhancer region (Fig.2C). Moreover, we divided the average span of the UNC5B-AS1

197   upstream promoter region into three segments (P1-P3, Fig.S1B) and performed ChIP-qPCR

198   experiments by using H3K27ac, H3K4me1, and FOXP3 antibodies. The results demonstrated

199   that FOXP3 has a strong binding affinity to segment P1 of the UNC5B-AS1 upstream promoter

200   region (Fig.2D). Coimmunoprecipitation confirmed the interaction among FOXP3, H3K27ac,

11

201 and H3K4me1 (Fig.2E). These findings confirmed that FOXP3 was recruited by the upstream

202 super enhancer E2 region and acted on the promoter P1 region of UNC5B-AS1, forming a

203 chromatin loop to regulate the expression of the super enhancer-driven lncRNA UNC5B-AS1.

204 **UNC5B-AS1 inhibits hypoxia-induced inflammatory phenotypic transition in PASMCs.**

205 To investigate the role of UNC5B-AS1 in hypoxic PH, we constructed an overexpression

206 plasmid for UNC5B-AS1 and validated its overexpression efficiency by RT-qPCR (Fig.S2A).

207 Subsequently, we overexpressed UNC5B-AS1 under hypoxic conditions and found that its

208 overexpression significantly inhibited the transition of hypoxia-induced PASMCs from a

209 contractile phenotype to a synthetic phenotype (Fig.3A, B and Fig.S2B). Inflammatory smooth

210 muscle cells actively secrete inflammatory cytokines such as IL-1β, IL-6, and TNF-α[29].

211 UNC5B-AS1 overexpression notably attenuated the hypoxia-induced inflammatory

212 phenotypic transition in PASMCs by suppressing the expression of IL-1β, IL-6, and TNF-α

213 (Fig.3C and Fig.S2C). These results confirm that UNC5B-AS1 alleviates the hypoxia-induced

214 inflammatory phenotypic transition in PASMCs.

215 **UNC5B-AS1 inhibits PASMCs proliferation by modulating inflammatory responses.**

216 Smooth muscle cells (SMCs) undergo phenotypic transition toward an inflammatory

217 phenotype and release inflammatory cytokines to participate in the perivascular inflammatory

218 microenvironment, ultimately leading to vascular remodeling[30]. To investigate the crucial role

219 of inflammatory PASMCs in the development of PH, we constructed a coculture system to

220 simulate the inflammatory microenvironment around blood vessels. First, PASMCs were

221 cultured under different experimental conditions for 24 hours. The cell culture supernatant

222 (conditioned medium, CM) was collected by centrifugation, and the levels of IL-1β, IL-6, and

223   TNF-α were measured. A portion of the remaining conditioned medium was mixed with normal

224   cell culture medium at a 1:1 ratio and used to stimulate normal PASMCs. Proliferation-related

225   markers were assessed after 24 hours to evaluate the impact of the inflammatory

226   microenvironment on normal PASMCs proliferation (Fig.S3A). Our results demonstrated that

227   UNC5B-AS1 overexpression significantly suppressed the secretion of IL-1β, IL-6, and TNF-α

228   in hypoxia-induced PASMCs (Fig.S3B). Conditioned media from UNC5B-AS1-

229   overexpressing cells significantly inhibited the proliferation (Fig.S3C) of normal PASMCs

230   under hypoxic conditions, which was accompanied by reduced cell viability (Fig.S3D) and

231   decreased expression of PCNA (Fig.S3E). These findings suggest that UNC5B-AS1 can

232   regulate the inflammatory microenvironment around blood vessels by suppressing the

233   inflammatory phenotypic transition of PASMCs, thereby alleviating hypoxia-induced PASMCs

234   proliferation.

235   **UNC5B-AS1 regulates the inflammatory microenvironment in hypoxia through**

236   **lactylation.**

237   The subcellular localization of lncRNAs determines their functions. We further examined

238   the subcellular localization of UNC5B-AS1. By using TOMM20 as a marker of mitochondria

239   and performing costaining with FISH, we found strong colocalization of UNC5B-AS1 with

240   mitochondria (Fig.4A). Subsequently, we isolated cytoplasm and mitochondria, RT-qPCR

241   showed the presence of UNC5B-AS1 in both compartments, and there was decreased

242   expression under hypoxic conditions (Fig.4B). Mitochondria, which are central organelles

243   involved in cellular energy metabolism, are closely related to glucose metabolism. Based on

244   the subcellular localization of UNC5B-AS1 and abnormal glucose metabolism under hypoxic

13

245 conditions, we further assessed the impact of UNC5B-AS1 on glycolysis, as in our previous

246 study[31]. Immunoblotting showed that UNC5B-AS1 overexpression inhibited the upregulation

247 of HKII and PKM2, which are key enzymes in glycolysis during hypoxia (Fig.4C). Lactate,

248 which is the main product of glycolysis, serves as a substrate for posttranslational modifications

249 of proteins[25]. Treatment of PASMCs with the glycolysis inhibitor 2-DG attenuated the hypoxia-

250 induced increase in protein lactylation and proliferation (Fig.S4A, B). Additionally, using

251 panlactylation antibody, we confirmed that UNC5B-AS1 overexpression abrogated the

252 increase in protein lactylation induced by hypoxia (Fig.4D). Finally, we assessed the H3K18la

253 levels of the promoters of the proinflammatory cytokines IL-1β, IL-6, and TNF-α. ChIP-qPCR

254 confirmed that UNC5B-AS1 modulated the lactylation levels of these gene promoters, thereby

255 affecting their expression (Fig.4E). These data suggest that UNC5B-AS1 affects the lactate

256 modification of the IL-1β, IL-6, and TNF-α promoter regions through the glycolysis pathway,

257 thereby increasing their expression and participating in the inflammatory phenotypic transition

258 of PASMCs.

259 **UNC5B-AS1 acts as a molecular scaffold to modulate the activity of mitochondrial**

260 **complex IV through LRPPRC.**

261   To further explore the specific mechanism by which UNC5B-AS1 influences the

262 glycolytic pathway, we used three bioinformatics websites (catRAPID, RNAct, and RNAInter)

263 and the subcellular localization of UNC5B-AS1 to identify LRPPRC as a downstream

264 mitochondrial-related protein associated with UNC5B-AS1 (Fig.S5A). Immunofluorescence

265 staining demonstrated that LRPPRC was localized within mitochondria, confirming its role as

266 a mitochondrial-related protein (Fig.S5B). The colocalization of UNC5B-AS1 and LRPPRC

267 was confirmed by FISH and immunofluorescence staining (Fig.5A). Immunoblotting indicated

268 that LRPPRC was downregulated under hypoxic conditions and that UNC5B-AS1 did not

269 influence its expression (Fig.5B). RNA Pull-down assays (Fig.5C) and RIP experiments

270 (Fig.5D) demonstrated the interaction between UNC5B-AS1 and LRPPRC. Based on these

271 findings, we confirmed the interaction between UNC5B-AS1 and LRPPRC, both of which are

272 associated with mitochondria, and the expression of LRPPRC was not affected by UNC5B-

273 AS1.

274 LRPPRC was reported to exert its biological effects by influencing the activity of

275 mitochondrial complex IV[32]. We propose that UNC5B-AS1 is a molecular scaffold between

276 LRPPRC and mitochondrial complex IV, facilitating their interaction and maintaining the

277 activity of mitochondrial complex IV. First, we designed small interfering RNAs (siRNA)

278 targeting UNC5B-AS1 and confirmed the efficiency of UNC5B-AS1 knockdown in PASMCs

279 (Fig.S5C). Immunoprecipitation showed that knockdown of UNC5B-AS1 affected the

280 interaction between mitochondrial complex IV and LRPPRC (Fig.5E). Subsequently, we

281 performed real-time monitoring of glycolysis using the Seahorse XFe24 extracellular flux

282 analyzer. As expected, knockout of UNC5B-AS1 activated glycolysis in PASMCs under

283 normoxic conditions, while overexpression of UNC5B-AS1 decreased glycolysis under

284 hypoxia-induced stress (Fig.5F). Next, we evaluated the impact of UNC5B-AS1 on the activity

285 of mitochondrial complex IV, and the results showed that knockdown of UNC5B-AS1 under

286 normoxic conditions impaired the activity of mitochondrial complex IV, while UNC5B-AS1

287 overexpression alleviated the hypoxia-induced decrease in the activity of mitochondrial

288 complex IV (Fig.5G). Finally, we assessed the effects of UNC5B-AS1 on lactate

15

289   dehydrogenase (LDH, catalyzing the conversion of pyruvate to lactate) activity and

290   intracellular lactate levels. The results confirmed that UNC5B-AS1 overexpression inhibited

291   the hypoxia-induced increase in LDH activity and intracellular lactate levels, while knockdown

292   of UNC5B-AS1 under normoxic conditions increased LDH activity (Fig.5H) and intracellular

293   lactate levels (Fig.5I). These findings confirm that UNC5B-AS1 acts as a molecular scaffold

294   between LRPPRC and mitochondrial complex IV, thereby regulating mitochondrial

295   metabolism and intracellular lactate production.

296   **The UNC5B-AS1 conserved fragment alleviates hypoxia-induced pulmonary**

297   **hypertension in vivo.**

298   To determine whether UNC5B-AS1 is functionally important in PH in vivo, we first used

299   the catRAPID tool to identify the functional fragment of UNC5B-AS1 that bound to LRPPRC

300   (Fig.S6A). We found a conserved sequence of this functional fragment in mice and named it

301   the UNC5B-AS1 conserved fragment (UA1CF, Fig.S6B). Subsequently, we validated the

302   expression of UA1CF in lung tissues of mice with SU5416 combined with hypoxia-induced

303   PH (SuHx mice) by using RT-qPCR and observed the downregulation of UA1CF expression

304   in SuHx mice (Fig.S6C). RIP experiments on mouse PASMCs confirmed the binding of

305   UA1CF with LRPPRC (Fig.S6D). Next, we constructed an adenovirus overexpressing UA1CF

306   and infected SuHx mice (Fig.6A). After hypoxic treatment, we assessed the impact of

307   adenoviral infection on mice by evaluating body weight and found that there was no significant

308   difference in body weight among the groups (Fig.S6E). RT-qPCR confirmed the successful

309   expression of UA1CF in mouse lung tissues (Fig.6B). We then evaluated SuHx-related PH

310   indicators in mice and found that UA1CF overexpression alleviated the increase in right

16

311　ventricular hypertrophy (Fig.6C) and right ventricular systolic pressure (RVSP, Fig.6D, E), as

312　well as the reduction in pulmonary artery acceleration time (PAAT, Fig.6F) and pulmonary

313　artery velocity-time integral (PAVTI, Fig.6G) in SuHx mice. However, it did not affect left

314　heart function in mice (Fig.6H). Histological analysis (H&E staining and Masson's trichrome

315　staining) revealed that UA1CF overexpression alleviated pulmonary arterial thickening and

316　perivascular fibrosis in SuHx mice (Fig.6I). These results confirm that UA1CF can alleviate

317　the symptoms of PH in SuHx mice.

318　**The UNC5B-AS1 conserved fragment alleviates pulmonary inflammation in PH mice.**

319　Next, we evaluated the impact of UA1CF on pulmonary lactate levels and the

320　inflammatory response in mice. UA1CF overexpression significantly alleviated the decrease in

321　mitochondrial complex IV activity (Fig.S7A) and the increases in LDH activity and lactate

322　levels (Fig.S7B-C) in the lung tissues of SuHx mice. Immunofluorescence staining of lung

323　tissues showed that UA1CF overexpression alleviated pulmonary arterial lactylation (Fig.S7D)

324　and IL-6 expression (Fig.S7E) in SuHx mice. ELISA showed that UA1CF overexpression

325　reduced the secretion of IL-1β, IL-6, and TNF-α in the lung tissues of SuHx mice (Fig.S7F).

326　These results indicate that UA1CF can alleviate the pulmonary inflammatory response in SuHx

327　mice.

328　**Discussion**

329　Previous studies have shown that UNC5B antisense lncRNA 1 (UNC5B-AS1) is involved

330　in and functionally relevant to a spectrum of biological events. This factor regulates signaling

331　pathways by acting as an RNA decoy and microRNA sponge[33], recruiting chromatin

332　modifiers[34] and inhibiting translation[35]. Recent studies have shown the involvement of

17

333 UNC5B-AS1 in various cancers, and it can influence the growth and metastasis of human colon

334 cancer cells by adsorbing miR-622 and ovarian cancer progression by regulating H3K27me on

335 NDRG2 via EZH2[34]. However, the role of UNC5B-AS1 in the cardiovascular or respiratory

336 systems, particularly in the pathogenesis of pulmonary arterial hypertension, remains unknown.

337 The present study comprehensively screened super enhancer (SE)-associated lncRNAs in PH

338 for the first time and showed that UNC5B-AS1 was driven by SEs in PASMCs. RNA-seq data

339 showed that UNC5B-AS1 was widely downregulated in PASMCs under hypoxic conditions,

340 while ChIP-seq and ChIP-qPCR assays identified UNC5B-AS1 as a super enhancer

341 transcriptional target that was directly occupied by both H3K27ac and H3K4me1. This result

342 was further verified by the finding that JQ1 (the BET bromodomain inhibitor) dramatically

343 suppressed the expression of UNC5B-AS1. Based on our findings, the identified landscape of

344 SEs may provide a better mechanistic understanding of the pathophysiological role of SE-

345 lncRNAs in PH.

346 SEs affect gene expression programs through the binding of transcription factors and

347 interactions with promoters[36]. To examine the precise factors that regulate UNC5B-AS1

348 expression in response to hypoxia, we analyzed the promoter of UNC5B-AS1 and found that

349 there were multiple binding sites for transcription factors, such as FOXP3, YY1, and USF2.

350 We observed that FOXP3 interacted with H3K27ac and H3K4me1 to maintain chromatin

351 looping between the UNC5B-AS1 promoter and its super enhancers and contributed to its

352 transcriptional activity in PASMCs. Although our data indicated that UNC5B-AS1 was

353 regulated by hypoxia in a FOXP3-dependent manner, whether other transcription factors and

354 epigenetic regulatory factors are involved in manipulating UNC5B-AS1 expression during

18

355   hypoxic conditions in PASMCs requires further analysis.

356   Lactylation can occur in various cellular contexts, and is particularly under low oxygen or

357   hypoxic conditions, catalyzed by lactate dehydrogenase enzymes[37]. Protein lactylation plays a

358   crucial role in diverse biological processes, including energy metabolism[38], cell signaling[39],

359   gene expression regulation[40], and cell growth[41]. For instance, in tumor-infiltrating myeloid

360   cells (TIMs), lactylation-driven METTL3-mediated RNA m6A modification enhances the

361   immunosuppressive capacity of TIMs[39]. Furthermore, in myocardial infarction, histone

362   lactylation regulates the dual activities of monocyte-derived macrophages by promoting the

363   transcription of the repair genes Lrg1, Vegf-α, and IL-10, thereby enabling anti-inflammatory

364   and proangiogenic responses[41]. Our research is the first report on the key role of lactylation in

365   the occurrence and development of PH. The SE-lncRNA UNC5B-AS1 plays a crucial role in

366   maintaining the contractile phenotype of PASMCs. Under hypoxic conditions, the loss of

367   UNC5B-AS1 decreases the binding of LRPPRC to mitochondrial complex IV, impairing its

368   activity and leading to aberrant activation of glycolysis, which ultimately causes intracellular

369   lactate accumulation in PASMCs. Excessive lactate in PASMCs leads to lactylation of the

370   upstream promoter regions of the IL-1β, IL-6, and TNF-α genes, thereby promoting the

371   transition of PASMCs toward an inflammatory phenotype. This results in the release of

372   inflammatory factors that participate in the vascular perivascular inflammatory

373   microenvironment. By overexpressing UNC5B-AS1 in cultured PASMCs, we further

374   demonstrated that the hypoxia-induced inflammatory phenotype in PASMCs and the release of

375   inflammatory factors occur in a UNC5B-AS1-dependent manner. These results indicate that

376   UNC5B-AS1 plays an important role in the development of pulmonary hypertension. Studying

19

377 the upstream lactylation sites on key genes and investigating the functions of their respective

378 writers, readers, and erasers in PH is important.

379 The interaction between lncRNAs and proteins has been shown to play an important role

380 in various biological processes. It has been reported that LRPPRC forms an RNA-dependent

381 protein complex that is necessary for maintaining a pool of nontranslated mRNAs in

382 mammalian mitochondria[42]. Studies have shown that the fibroblasts and skeletal muscle

383 homogenates of mitochondrial disease patients showed decreased protein levels of LRPPRC

384 and impaired complex IV enzyme activity, which were associated with abnormal complex

385 assembly and reduced steady-state levels of numerous oxidative phosphorylation subunits[43].

386 The lncRNA SNHG17 has been shown to stabilize c-Myc protein and promote G1/S transition

387 and cell proliferation by interacting with LRPPRC[44]. It can be hypothesized that LRPPRC is

388 crucial for maintaining mitochondrial oxidative respiratory chain activity and is capable of

389 binding to lncRNAs to exert biological effect. Our present study showed that UNC5B-AS1

390 could act as an LRPPRC molecular scaffold, thereby interfering with mitochondrial complex

391 IV to modulate oxidative phosphorylation. These findings suggest that UNC5B-AS1 regulates

392 glycolysis by modulating LRPPRC and mitochondrial complex IV. Ultimately, through

393 lactylation, UNC5B-AS1 affects the perivascular inflammatory microenvironment and the

394 inflammatory phenotypic transition of PASMCs, indicating that UNC5B-AS1 overexpression

395 may provide therapeutic options for PH.

396 The highly conserved region of UNC5B-AS1 that binds to LRPPRC functional fragment

397 was identified using bioinformatics tools in the mouse genome. We found that the expression

398 of the UNC5B-AS1 conserved fragment named UA1CF was absent in the lung tissues of PH

399 mice induced by SU5416 combined with hypoxia (SuHx). Additionally, in mouse PASMCs,

400 UA1CF could bind to LRPPRC. Adenovirus infectionwas used to overexpress UA1CF in the

401 lungs of mice. We discovered that UA1CF could alleviate the symptoms of PH induced by

402 SuHx in mice. Similarly, UA1CF expression in mouse lung tissues influenced the activity of

403 mitochondrial complex IV, as well as the lactate levels and the extent of panlactylation

404 modification in the lungs. Finally, we evaluated the levels of the inflammatory factors IL-1β,

405 IL-6, and TNF-α, in mouse lung tissues and found that UA1CF significantly alleviated

406 pulmonary inflammation in PH mice. Based on these results, we confirmed that UA1CF could

407 alleviate the symptoms of PH and the levels of pulmonary inflammation in SuHx mice and

408 provided substantial evidence supporting the beneficial role of UNC5B-AS1 in PH.

409 Furthermore, it would be interesting to further investigate whether UA1CF was part of another

410 novel lncRNA in the mouse genome.

411   In conclusion, the present study demonstrated that the SE-driven lncRNA UNC5B-AS1

412 plays a vital role in alleviating the inflammatory phenotype of PASMCs, thereby regulating the

413 pathological remodeling of vessels in PH. Mechanistically, UNC5B-AS1 functioned as a novel

414 checkpoint molecule in oxidative phosphorylation by acting as an LRPPRC molecular scaffold,

415 thereby modulating the activity of mitochondrial complex IV. Downregulation of UNC5B-AS1

416 reduced the binding of LRPPRC to mitochondrial complex IV, leading to increased lactic acid

417 levels and promoting lactylation of the promoter regions of IL-1β, IL-6, and TNF-α, thereby

418 contributing to a perivascular inflammatory microenvironment that stimulates the proliferation

419 of surrounding PASMCs. This finding implicates SE-lncRNAs in PH and suggests that the

420 modulation of UNC5B-AS1 activity and its downstream targets, such as LRPPRC, is a novel

421 therapeutic approach for treating this hypoxia-associated disease.

422 **Acknowledgments**

423 X.Z. designed the research, performed the experiments, analyzed the results, and wrote the

424 manuscript. X.Z., X.W., X.G., L.Z., Z.W., X.P., J.M., L.O., Z.M., and Y.L. performed the

425 experiments and analyzed the results. X.W., and C.M. performed and analyzed the RNA

426 sequencing and ChIP sequencing, supervised the research, and wrote the manuscript. X.Z., and

427 Y.C. supervised the study. F.L. and X.Z. performed the animal experiments and interpreted the

428 results. C.M. designed and supervised the research and approved the final version of the

429 manuscript.

430 **Sources of Funding**

435 **Disclosures**

436 None.

437 **Supplemental Material**

438 Supplemental Methods

439 Tables S1-S4

440 Figure S1-S7

441

References

1. Morrell NW, Adnot S, Archer SL, Dupuis J, Lloyd Jones P, MacLean MR, McMurtry IF, Stenmark KR, Thistlethwaite PA, Weissmann N, et al. Cellular and molecular basis of pulmonary arterial hypertension. *J Am Coll Cardiol*. 2009;54:S20-S31. doi: 10.1016/j.jacc.2009.04.018

2. Voelkel NF, Tuder RM. Hypoxia-induced pulmonary vascular remodeling: a model for what human disease? *J Clin Invest*. 2000;106:733-738. doi: 10.1172/JCI11144

3. Fedullo PF, Auger WR, Kerr KM, Rubin LJ. Chronic thromboembolic pulmonary hypertension. *N Engl J Med*. 2001;345:1465-1472. doi: 10.1056/NEJMra010902

4. Li D, Shao NY, Moonen JR, Zhao Z, Shi M, Otsuki S, Wang L, Nguyen T, Yan E, Marciano DP, et al. ALDH1A3 Coordinates Metabolism With Gene Regulation in Pulmonary Arterial Hypertension. *Circulation*. 2021;143:2074-2090. doi: 10.1161/CIRCULATIONAHA.120.048845

5. Ruffenach G, Medzikovic L, Aryan L, Li M, Eghbali M. HNRNPA2B1: RNA-Binding Protein That Orchestrates Smooth Muscle Cell Phenotype in Pulmonary Arterial Hypertension. *Circulation*. 2022;146:1243-1258. doi: 10.1161/CIRCULATIONAHA.122.059591

6. Hecker M, Zaslona Z, Kwapiszewska G, Niess G, Zakrzewicz A, Hergenreider E, Wilhelm J, Marsh LM, Sedding D, Klepetko W, et al. Dysregulation of the IL-13 receptor system: a novel pathomechanism in pulmonary arterial hypertension. *Am J Respir Crit Care Med*. 2010;182:805-818. doi: 10.1164/rccm.200909-1367OC

7. Omura J, Satoh K, Kikuchi N, Satoh T, Kurosawa R, Nogi M, Ohtsuki T, Al-Mamun

ME, Siddique MAH, Yaoita N, et al. ADAMTS8 Promotes the Development of Pulmonary Arterial Hypertension and Right Ventricular Failure: A Possible Novel Therapeutic Target. *Circ Res*. 2019;125:884-906. doi: 10.1161/CIRCRESAHA.119.315398

8. Xiao Y, Christou H, Liu L, Visner G, Mitsialis SA, Kourembanas S, Liu H. Endothelial indoleamine 2,3-dioxygenase protects against development of pulmonary hypertension. *Am J Respir Crit Care Med*. 2013;188:482-491. doi: 10.1164/rccm.201304-0700OC

9. Chen T, Huang JB, Dai J, Zhou Q, Raj JU, Zhou G. PAI-1 is a novel component of the miR-17~92 signaling that regulates pulmonary artery smooth muscle cell phenotypes. *Am J Physiol Lung Cell Mol Physiol*. 2018;315:L149-L161. doi: 10.1152/ajplung.00137.2017

10. Parpaleix A, Amsellem V, Houssaini A, Abid S, Breau M, Marcos E, Sawaki D, Delcroix M, Quarck R, Maillard A, et al. Role of interleukin-1 receptor 1/MyD88 signalling in the development and progression of pulmonary hypertension. *Eur Respir J*. 2016;48:470-483. doi: 10.1183/13993003.01448-2015

11. Kapranov P, Cheng J, Dike S, Nix DA, Duttagupta R, Willingham AT, Stadler PF, Hertel J, Hackermuller J, Hofacker IL, et al. RNA maps reveal new RNA classes and a possible function for pervasive transcription. *Science*. 2007;316:1484-1488. doi: 10.1126/science.1138341

12. Wang Y, Chen W, Lian J, Zhang H, Yu B, Zhang M, Wei F, Wu J, Jiang J, Jia Y, et al. The lncRNA PVT1 regulates nasopharyngeal carcinoma cell proliferation via activating the KAT2A acetyltransferase and stabilizing HIF-1alpha. *Cell Death Differ*.

486   2020;27:695-710. doi: 10.1038/s41418-019-0381-y

487   13.   Wang Z, Chen X, Liu N, Shi Y, Liu Y, Ouyang L, Tam S, Xiao D, Liu S, Wen F, et al.

488   A Nuclear Long Non-Coding RNA LINC00618 Accelerates Ferroptosis in a Manner

489   Dependent   upon   Apoptosis.   *Mol   Ther*.   2021;29:263-274.   doi:

490   10.1016/j.ymthe.2020.09.024

491   14.   Zhang L, Li C, Su X. Emerging impact of the long noncoding RNA MIR22HG on

492   proliferation and apoptosis in multiple human cancers. *J Exp Clin Cancer Res*.

493   2020;39:271. doi: 10.1186/s13046-020-01784-8

494   15.   Ni W, Zhang Y, Zhan Z, Ye F, Liang Y, Huang J, Chen K, Chen L, Ding Y. A novel

495   lncRNA uc.134 represses hepatocellular carcinoma progression by inhibiting CUL4A-

496   mediated ubiquitination of LATS1. *J Hematol Oncol*. 2017;10:91. doi: 10.1186/s13045-

497   017-0449-4

498   16.   Yu J, Wang W, Yang J, Zhang Y, Gong X, Luo H, Cao N, Xu Z, Tian M, Yang P, et al.

499   LncRNA PSR Regulates Vascular Remodeling Through Encoding a Novel Protein

500   Arteridin. *Circ Res*. 2022;131:768-787. doi: 10.1161/CIRCRESAHA.122.321080

501   17.   Tan YT, Lin JF, Li T, Li JJ, Xu RH, Ju HQ. LncRNA-mediated posttranslational

502   modifications and reprogramming of energy metabolism in cancer. *Cancer Commun*

503   *(Lond)*. 2021;41:109-120. doi: 10.1002/cac2.12108

504   18.   Huang D, Chen J, Yang L, Ouyang Q, Li J, Lao L, Zhao J, Liu J, Lu Y, Xing Y, et al.

505   NKILA lncRNA promotes tumor immune evasion by sensitizing T cells to activation-

506   induced cell death. *Nat Immunol*. 2018;19:1112-1125. doi: 10.1038/s41590-018-0207-

507   y

19. Whyte WA, Orlando DA, Hnisz D, Abraham BJ, Lin CY, Kagey MH, Rahl PB, Lee TI, Young RA. Master transcription factors and mediator establish super-enhancers at key cell identity genes. *Cell*. 2013;153:307-319. doi: 10.1016/j.cell.2013.03.035

20. Bian E, Chen X, Cheng L, Cheng M, Chen Z, Yue X, Zhang Z, Chen J, Sun L, Huang K, et al. Super-enhancer-associated TMEM44-AS1 aggravated glioma progression by forming a positive feedback loop with Myc. *J Exp Clin Cancer Res*. 2021;40:337. doi: 10.1186/s13046-021-02129-9

21. Zhang H, Xu R, Li B, Xin Z, Ling Z, Zhu W, Li X, Zhang P, Fu Y, Chen J, et al. LncRNA NEAT1 controls the lineage fates of BMSCs during skeletal aging by impairing mitochondrial function and pluripotency maintenance. *Cell Death Differ*. 2022;29:351-365. doi: 10.1038/s41418-021-00858-0

22. Dong K, Shen J, He X, Hu G, Wang L, Osman I, Bunting KM, Dixon-Melvin R, Zheng Z, Xin H, et al. CARMN Is an Evolutionarily Conserved Smooth Muscle Cell-Specific LncRNA That Maintains Contractile Phenotype by Binding Myocardin. *Circulation*. 2021;144:1856-1875. doi: 10.1161/CIRCULATIONAHA.121.055949

23. Zhang D, Tang Z, Huang H, Zhou G, Cui C, Weng Y, Liu W, Kim S, Lee S, Perez-Neut M, et al. Metabolic regulation of gene expression by histone lactylation. *Nature*. 2019;574:575-580. doi: 10.1038/s41586-019-1678-1

24. Ivashkiv LB. The hypoxia-lactate axis tempers inflammation. *Nat Rev Immunol*. 2020;20:85-86. doi: 10.1038/s41577-019-0259-8

25. Pan RY, He L, Zhang J, Liu X, Liao Y, Gao J, Liao Y, Yan Y, Li Q, Zhou X, et al. Positive feedback regulation of microglial glucose metabolism by histone H4 lysine 12

lactylation in Alzheimer's disease. *Cell Metab*. 2022;34:634-648 e636. doi: 10.1016/j.cmet.2022.02.013

26. Irizarry-Caro RA, McDaniel MM, Overcast GR, Jain VG, Troutman TD, Pasare C. TLR signaling adapter BCAP regulates inflammatory to reparatory macrophage transition by promoting histone lactylation. *Proc Natl Acad Sci U S A*. 2020;117:30628-30638. doi: 10.1073/pnas.2009778117

27. Ma C, Li Y, Ma J, Liu Y, Li Q, Niu S, Shen Z, Zhang L, Pan Z, Zhu D. Key role of 15-lipoxygenase/15-hydroxyeicosatetraenoic acid in pulmonary vascular remodeling and vascular angiogenesis associated with hypoxic pulmonary hypertension. *Hypertension*. 2011;58:679-688. doi: 10.1161/HYPERTENSIONAHA.111.171561

28. Ma C, Wang X, He S, Zhang L, Bai J, Qu L, Qi J, Zheng X, Zhu X, Mei J, et al. Ubiquitinated AIF is a major mediator of hypoxia-induced mitochondrial dysfunction and pulmonary artery smooth muscle cell proliferation. *Cell Biosci*. 2022;12:9. doi: 10.1186/s13578-022-00744-3

29. Wang J, Xie SA, Li N, Zhang T, Yao W, Zhao H, Pang W, Han L, Liu J, Zhou J. Matrix stiffness exacerbates the proinflammatory responses of vascular smooth muscle cell through the DDR1-DNMT1 mechanotransduction axis. *Bioact Mater*. 2022;17:406-424. doi: 10.1016/j.bioactmat.2022.01.012

30. Viswanathan G, Kirshner HF, Nazo N, Ali S, Ganapathi A, Cumming I, Zhuang Y, Choi I, Warman A, Jassal C, et al. Single-Cell Analysis Reveals Distinct Immune and Smooth Muscle Cell Populations that Contribute to Chronic Thromboembolic Pulmonary Hypertension. *Am J Respir Crit Care Med*. 2023;207:1358-1375. doi:

552   10.1164/rccm.202203-0441OC

553   31.   Ma C, Wang X, Zhang L, Zhu X, Bai J, He S, Mei J, Jiang J, Guan X, Zheng X, et al.

554   Super Enhancer-Associated Circular RNA-CircKrt4 Regulates Hypoxic Pulmonary

555   Artery Endothelial Cell Dysfunction in Mice. *Arterioscler Thromb Vasc Biol*.

556   2023;43:1179-1198. doi: 10.1161/ATVBAHA.122.318842

557   32.   Cooper MP, Qu L, Rohas LM, Lin J, Yang W, Erdjument-Bromage H, Tempst P,

558   Spiegelman BM. Defects in energy homeostasis in Leigh syndrome French Canadian

559   variant through PGC-1alpha/LRP130 complex. *Genes Dev*. 2006;20:2996-3009. doi:

560   10.1101/gad.1483906

561   33.   Zhang Y, Li Z, Lan Z. Silencing UNC5B antisense lncRNA 1 represses growth and

562   metastasis of human Colon cancer cells via raising miR-622. *Artif Cells Nanomed*

563   *Biotechnol*. 2020;48:60-67. doi: 10.1080/21691401.2019.1699809

564   34.   Wang H, Su H, Tan Y. UNC5B-AS1 promoted ovarian cancer progression by regulating

565   the H3K27me on NDRG2 via EZH2. *Cell Biol Int*. 2020;44:1028-1036. doi:

566   10.1002/cbin.11300

567   35.   Tan SF, Ni JX, Xiong H. LncRNA UNC5B-AS1 promotes malignant progression of

568   prostate cancer by competitive binding to caspase-9. *Eur Rev Med Pharmacol Sci*.

569   2020;24:2271-2280. doi: 10.26355/eurrev_202003_20493

570   36.   Bal E, Kumar R, Hadigol M, Holmes AB, Hilton LK, Loh JW, Dreval K, Wong JCH,

571   Vlasevska S, Corinaldesi C, et al. Super-enhancer hypermutation alters oncogene

572   expression in B cell lymphoma. *Nature*. 2022;607:808-815. doi: 10.1038/s41586-022-

573   04906-8

574   37.   Li X, Yang Y, Zhang B, Lin X, Fu X, An Y, Zou Y, Wang JX, Wang Z, Yu T. Lactate

575   metabolism in human health and disease. *Signal Transduct Target Ther*. 2022;7:305.

576   doi: 10.1038/s41392-022-01151-3

577   38.   Liberti MV, Locasale JW. Histone Lactylation: A New Role for Glucose Metabolism.

578   *Trends Biochem Sci*. 2020;45:179-182. doi: 10.1016/j.tibs.2019.12.004

579   39.   Xiong J, He J, Zhu J, Pan J, Liao W, Ye H, Wang H, Song Y, Du Y, Cui B, et al.

580   Lactylation-driven   METTL3-mediated   RNA   m(6)A   modification   promotes

581   immunosuppression of tumor-infiltrating myeloid cells. *Mol Cell*. 2022;82:1660-1677

582   e1610. doi: 10.1016/j.molcel.2022.02.033

583   40.   Galle E, Wong CW, Ghosh A, Desgeorges T, Melrose K, Hinte LC, Castellano-Castillo

584   D, Engl M, de Sousa JA, Ruiz-Ojeda FJ, et al. H3K18 lactylation marks tissue-specific

585   active enhancers. *Genome Biol*. 2022;23:207. doi: 10.1186/s13059-022-02775-y

586   41.   Wang N, Wang W, Wang X, Mang G, Chen J, Yan X, Tong Z, Yang Q, Wang M, Chen

587   L, et al. Histone Lactylation Boosts Reparative Gene Activation Post-Myocardial

588   Infarction. *Circ Res*. 2022;131:893-908. doi: 10.1161/CIRCRESAHA.122.320488

589   42.   Mili S, Pinol-Roma S. LRP130, a pentatricopeptide motif protein with a noncanonical

590   RNA-binding domain, is bound in vivo to mitochondrial and nuclear RNAs. *Mol Cell*

591   *Biol*. 2003;23:4972-4982. doi: 10.1128/MCB.23.14.4972-4982.2003

592   43.   Olahova M, Hardy SA, Hall J, Yarham JW, Haack TB, Wilson WC, Alston CL, He L,

593   Aznauryan E, Brown RM, et al. LRPPRC mutations cause early-onset multisystem

594   mitochondrial   disease   outside   of   the   French-Canadian   population.   *Brain*.

595   2015;138:3503-3519. doi: 10.1093/brain/awv291

44. Liu JY, Chen YJ, Feng HH, Chen ZL, Wang YL, Yang JE, Zhuang SM. LncRNA SNHG17 interacts with LRPPRC to stabilize c-Myc protein and promote G1/S transition and cell proliferation. *Cell Death Dis*. 2021;12:970. doi: 10.1038/s41419-021-04238-x

Highlights:

The long non-coding RNA UNC5B-AS1, regulated by super-enhancers (SE), is downregulated in hypoxic PASMCs, and regulates PASMC phenotype transition through glycolysis.

The super-enhancer region of lncRNA UNC5B-AS1 recruits the transcription factor FOXP3 to its promoter region, forming a chromatin loop to regulate its expression.

The lncRNA UNC5B-AS1 acts as a molecular scaffold stabilizing the interaction between LRPPRC and mitochondrial complex IV.

The lactate generated by glycolysis activation induces lactylation modification of histones at the IL-1β, IL-6, and TNF-α promoters, leading to the inflammatory phenotype transition of PASMCs.

Overexpression of lncRNA UNC5B-AS1 conserved fragment reversed SuHx-induced PH in mice.

Figures with Figure Legends
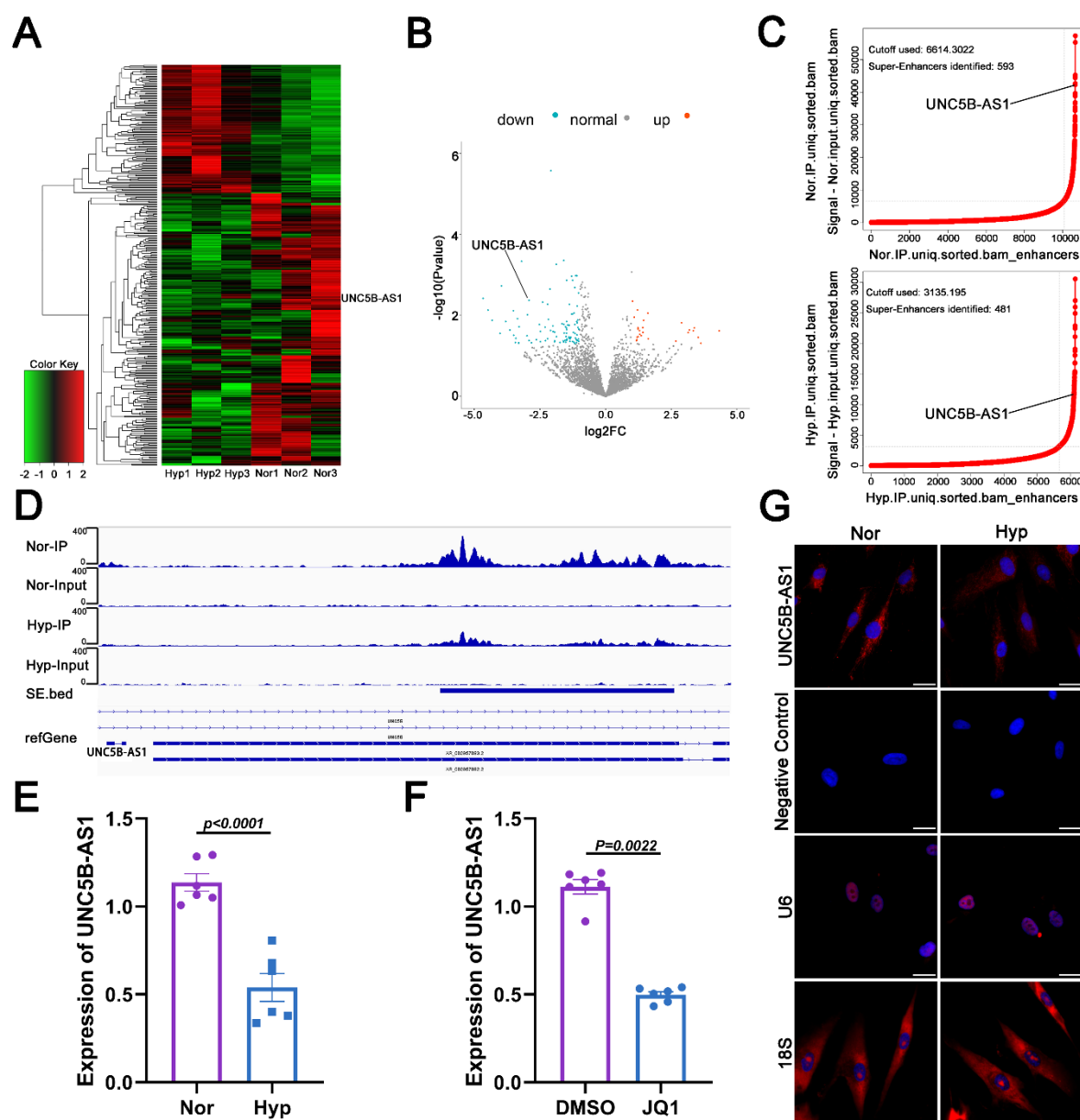
Fig.1 The super enhancer-driven lncRNA UNC5B-AS1 is downregulated in hypoxic PASMCs.

A The heatmap displays the differentially expressed genes identified in normoxic/hypoxic PASMCs based on RNA-seq analysis (n=3). **B** The RNA-seq results are visualized as a volcano plot, displaying the expression pattern of UNC-5B-AS1 in normoxic/hypoxic PASMCs. **C** The hockey stick plot displays the activity of super enhancers and enhancers upstream of UNC5B-

31

621   AS1 in normoxic/hypoxic PASMCs (Super enhancers are defined as slope >1, while enhancers

622   slope <1). **D** To visualize the enrichment profile of H3K27ac signal peaks upstream of UNC5B-

623   AS1 in normoxic/hypoxic PASMCs by using IGV (Integrative Genomics Viewer). **E** The

624   expression levels of UNC5B-AS1 in normoxic/hypoxic PASMCs (n=6). **F** The expression

625   levels of UNC5B-AS1 after treatment of PASMCs with JQ1 (n=6). Statistical comparison was

626   performed by the paired Student's t test (two-sided). **G** FISH results for the localization of

627   UNC5B-AS1 in normoxic/hypoxic PASMCs. Scale bars=50μm. All data are presented as mean

628   ± SEM. Nor, normoxia and Hyp, hypoxia.

629
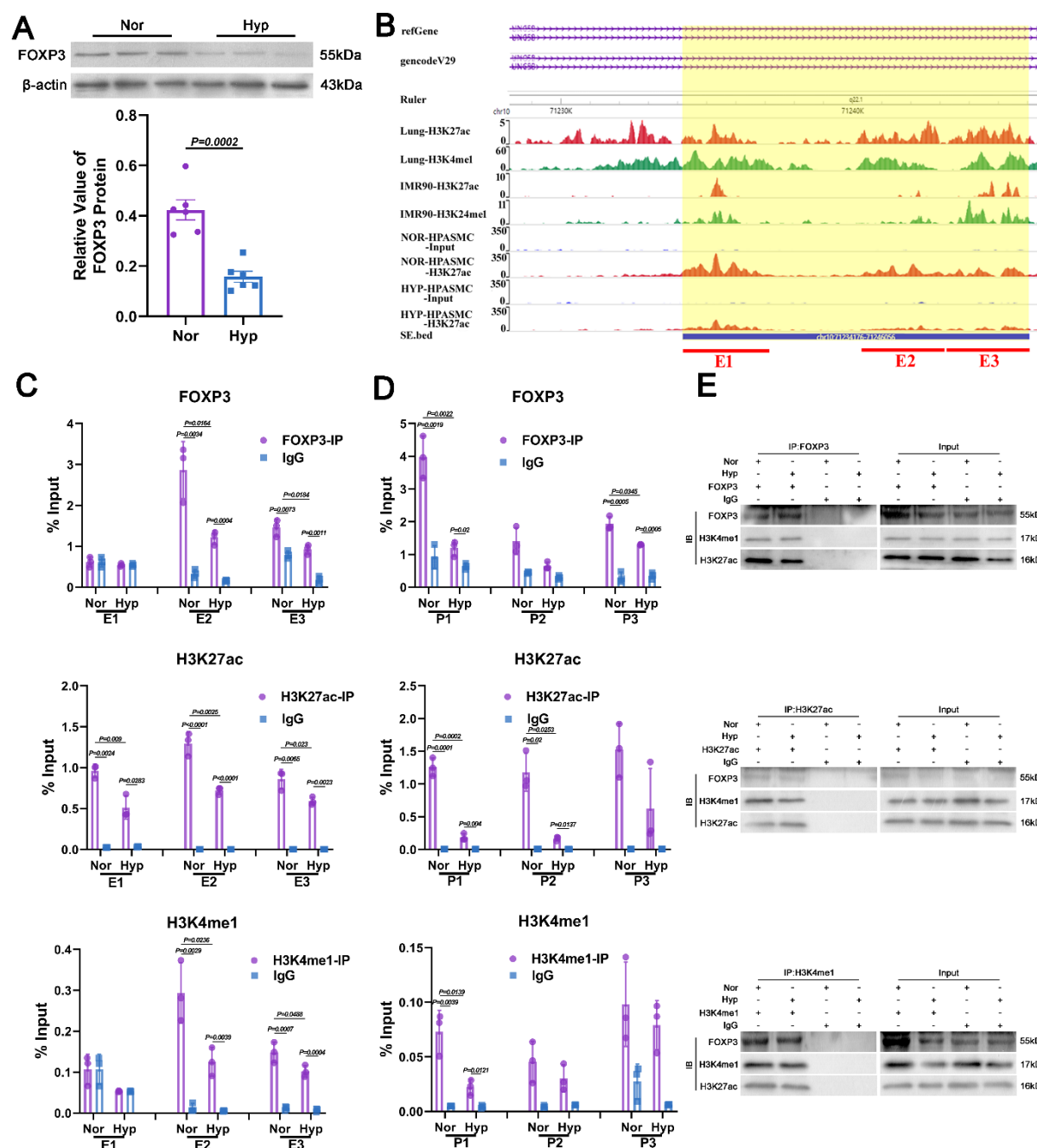
Fig.2 FOXP3 regulates the expression of UNC5B-AS1 through chromatin remodeling.

A Western blot analysis of FOXP3 in normoxic/hypoxic PASMCs (n=6). **B** Schematic diagram illustrating the segmentation of the upstream super enhancer region of UNC5B-AS1 based on H3K27ac ChIP-seq results. FOXP3, H3K27ac, and H3K4me1 ChIP-qPCR results showing their enrichment in the upstream super enhancer region (**C**) and promoter region (**D**) of UNC5B-AS1 (n=3). **E** Results of co-immunoprecipitation with FOXP3, H3K27ac, and

33

637   H3K4me1. Statistical comparison was performed by the paired Student's t test (two-sided). All

638   data are presented as mean ± SEM. Nor, normoxia, Hyp, hypoxia, P, promoter, E, super

639   enhancer, IP, immunoprecipitation, IB, Immunoblotting and IgG, Immunoglobulin G.

640
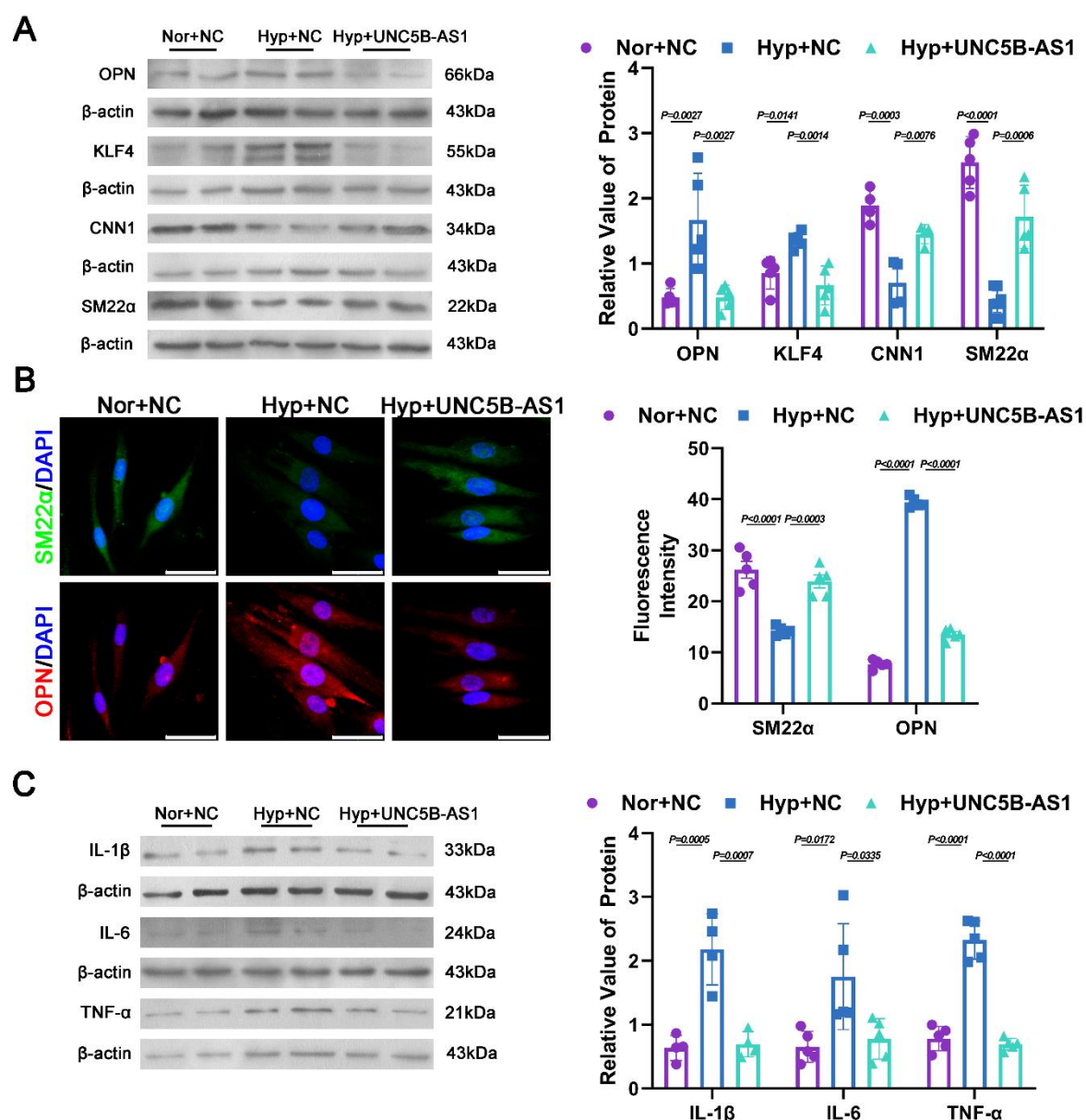
Fig.3 UNC5B-AS1 alleviates hypoxia-induced inflammatory phenotypic transition in PASMCs.

A Western blot analysis of OPN, KLF4, CNN1 and SM22α in PASMCs (n=5 for OPN, KLF4 and SM22α, n=4 for CNN1). **B** Representative immunofluorescence images of PASMCs stained with anti-SM22α (green) antibody, anti-OPN (red) antibody and DAPI (blue). Scale bars=100 μm. **C** Western blot analysis of IL-1β, IL-6 and TNF-α in PASMCs (n=5 for IL-6 and TNF-α, n=4 for IL-1β). All data are presented as mean ± SEM. One-way ANOVA with Tukey

649   post hoc test was used to compare multiple groups with equal variance, and Brown-Forsythe

650   and Welch ANOVA with Tamhane T2 post hoc test was used to compare multiple groups with

651   unequal variance. Nor, normoxia, Hyp, hypoxia, NC, Negative control and UNC5B-AS1,
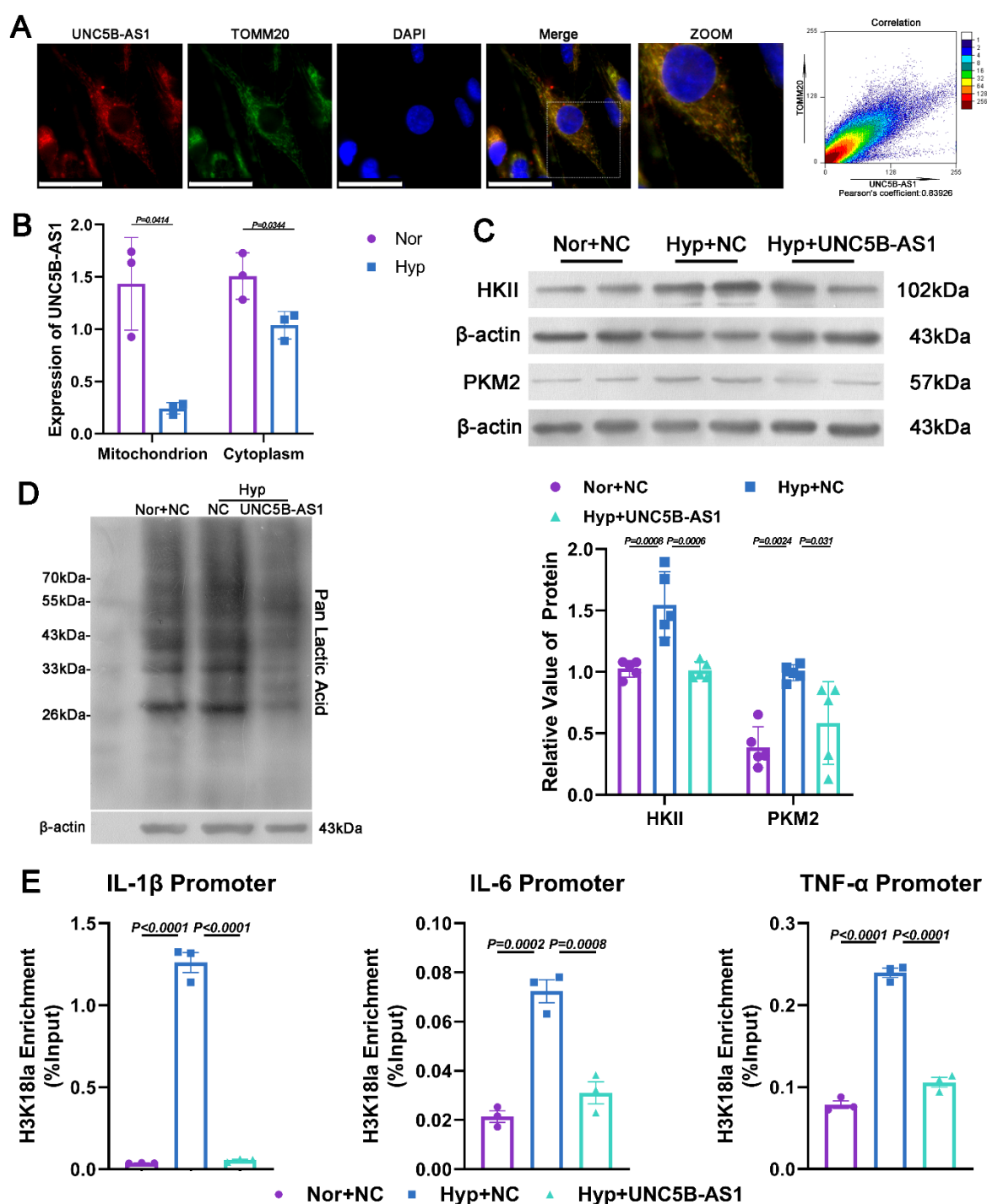
652   UNC5B-AS1 overexpression.

653

Fig.4 UNC5B-AS1 inhibits the expression of inflammatory factors through lactylation modification.

A Representative immunofluorescence images of PASMCs stained with anti-TOMM20 (green) antibody, UNC5B-AS1 probe (red) and DAPI (blue), the Pearson correlation coefficient reflects the correlation between two fluorescence labels in co-localization. Scale bars=100 μm.

37

660 **B** Expression of UNC5B-AS1 in PASMC mitochondrion and cytoplasm (n=3). Statistical

661 comparison was performed by the paired Student's t test (two-sided). **C** Western blot analysis

662 of the expression of HKII and PKM2 in PASMCs (n=5). **D** Western blot analysis of pan-

663 lactylation modification in PASMCs. **E** ChIP-qPCR analysis of H3K18la modification in IL-

664 1β, IL-6 and TNF-α promoter (n=3). All data are presented as mean ± SEM. One-way ANOVA

665 with Tukey post hoc test was used to compare multiple groups with equal variance, and Brown-

666 Forsythe and Welch ANOVA with Tamhane T2 post hoc test was used to compare multiple

667 groups with unequal variance. Nor, normoxia, Hyp, hypoxia, NC, Negative control and
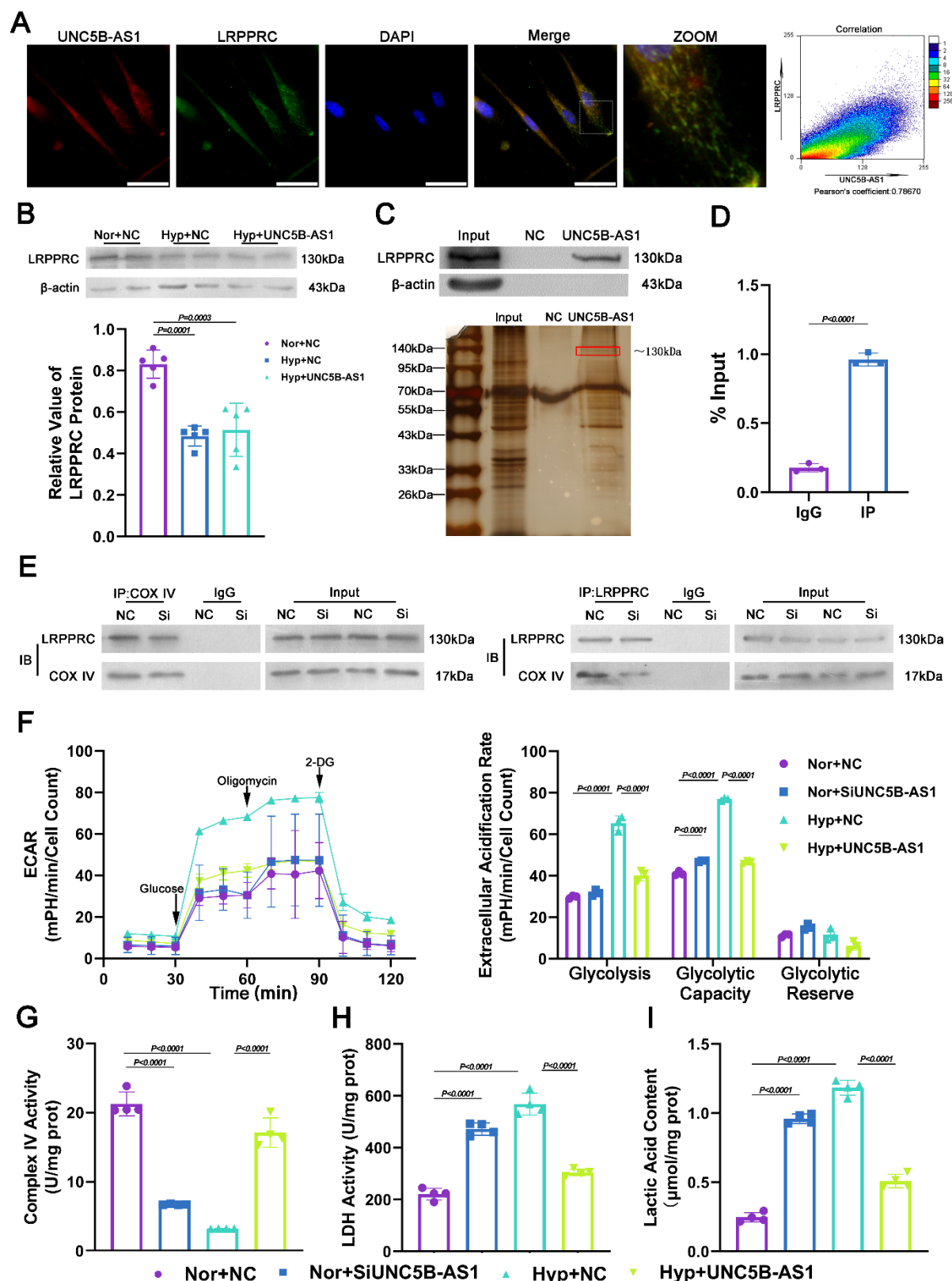
668 UNC5B-AS1, UNC5B-AS1 overexpression.

669

Fig.5 UNC5B-AS1 acts as a molecular scaffold by binding to LRPPRC, influencing the

activity of mitochondrial complex IV.

670

671

A Representative immunofluorescence images of PASMCs stained with anti-LRPPRC (green) antibody, UNC5B-AS1 probe (red) and DAPI (blue), the Pearson correlation coefficient reflects the correlation between two fluorescence labels in co-localization. Scale bars=100 μm. **B** Western blot analysis of LRPPRC in PASMCs (n=5). **C** Up panel, RNA pull-down analysis was performed to examine the binding between UNC5B-AS1 and LRPPRC in PASMCs. Below panel, silver staining results of RNA Pull-down in PASMCs. **D** RIP analysis was performed to examine the binding between UNC5B-AS1 and LRPPRC in PASMCs (n=3). Statistical comparison was performed by the paired Student's t test (two-sided). **E** Results of co-immunoprecipitation with mitochondrial complex IV (COX IV) and LRPPRC after siUNC5B-AS1. **F** Glycolysis and glycolytic reserve following treatment with 10 mmol/L glucose and 1 μM oligomycin were measured in cultured PASMCs, and nonglycolytic acidification after treatment with 100 mmol/L 2-deoxyglucose was detected (n=3). Mitochondrial complex IV activity (**G**), LDH activity (**H**) and intracellular lactic acid contents (**I**) in PASMCs (n=4). All data are presented as mean ± SEM. One-way ANOVA with Tukey post hoc test was used to compare multiple groups with equal variance, and Brown-Forsythe and Welch ANOVA with Tamhane T2 post hoc test was used to compare multiple groups with unequal variance. Nor, normoxia, Hyp, hypoxia, NC, Negative control, SiUNC5B-AS1, UNC5B-AS1 small interfering RNA and UNC5B-AS1, UNC5B-AS1 overexpression.
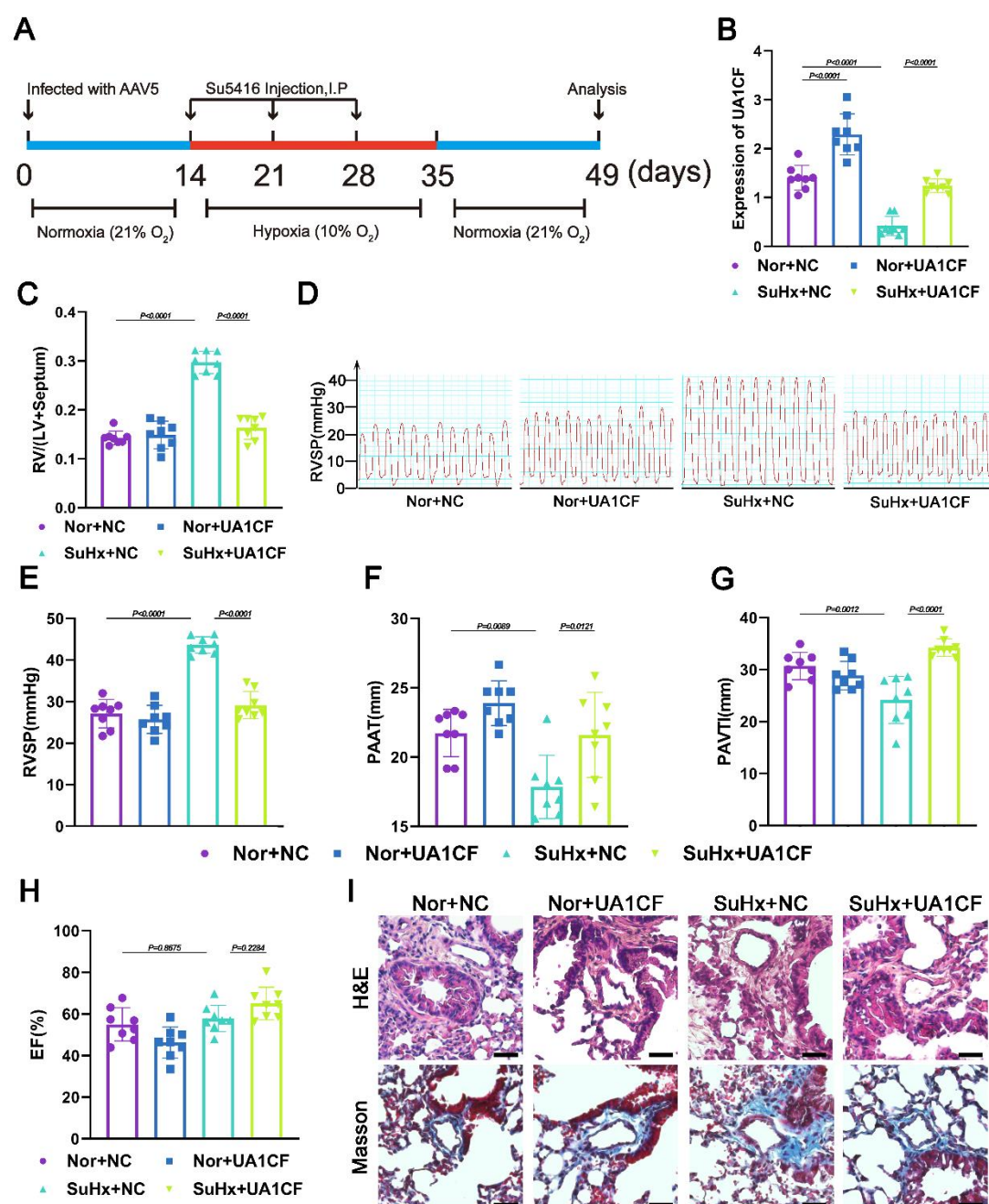
Fig. 6 UNC5B-AS1 conserved fragment alleviates SuHx-induced PH in mice.

A Schematic diagram of the SU5416 combined with hypoxia-induced PH (SuHx) mice model.

B Expression of UNC5B-AS1 conserved fragment (UA1CF) in mice lungs (n=8). **C** Right

ventricle/left ventricle + septum (RV/LV+ Septum) in mice (n=8). **D** Representative waveform

of right ventricular systolic pressure. **E** Representative right ventricular systolic pressure

(RVSP) in mice (n=8). Pulmonary artery acceleration time (PAAT, **F**), pulmonary artery

697   velocity-time integral (PAVTI, **G**), ejection fraction (EF, **H**) in mice (n=8). **I** Representative

698   images of Hematoxylin and Eosin staining (H&E) and Masson staining in mice lungs. Scale

699   bars=50 μm. All data are presented as mean ± SEM. One-way ANOVA with Tukey post hoc

700   test was used to compare multiple groups with equal variance, and Brown-Forsythe and Welch

701   ANOVA with Tamhane T2 post hoc test was used to compare multiple groups with unequal

702   variance. Nor, normoxia, SuHx, SU5416 combined with hypoxia, NC, Negative control and

703   UA1CF, AAV5-UNC5B-AS1 conserved fragment overexpression.